Computer Science Department Technical Report
University of California
Los Angeles, CA 90024-1596

DELAY ESTIMATION OF TREES USING TWO-POLE METHODS AND OPTIMAL EQUIVALENT CIRCUITS

A. B. Kahng
S. Muddu

October 1993
CSD-930035

Delay Estimation of Trees Using Two-Pole Methods and Optimal Equivalent Circuits *

Andrew B. Kahng and Sudhakar Muddu

UCLA Computer Science Department, Los Angeles, CA 90024-1596 USA
abk@cs.ucla.edu, sudhakar@cs.ucla.edu

Abstract

Performance-driven interconnect design is a major concern in the synthesis of VLSI systems. Delay estimation models are crucial in determining both the topology and the layout of good routing trees. In this paper, we address the class of *moment-matching*, or *moment representation*, methods which have been used for the simulation of interconnects that are modeled as distributed *RC* or *RLC* lines. We provide new *optimal* 2- and 3-segment equivalent circuits for the distributed *RLC* and distributed *RC* models. Our equivalent circuits approximate a distributed *RLC* structure accurately up to second degree terms, i.e., we obtain the exact first and second moments, and the third moment is almost exact. We have assessed the significance of our contribution by using a two-pole methodology to calculate the voltage response. Our results show that the previous approximate two-pole methods are off by at least 18%, even for the small test cases studied in previous papers. As routing trees become bigger and interconnection lines become longer, the advantage of our approach over previous approximate methods, both in accuracy and simulation complexity, becomes highly significant. The improved accuracy afforded by our results is particularly important for the design of high-speed systems.

1 Introduction

Accurate calculation of propagation delay in VLSI interconnects is critical to the design of high speed systems and to performance-driven routing. Direct simulation codes such as SPICE can be used for the simulation of any circuit, but cannot provide either the efficiency or the physical intuition needed for layout design. At the same time, simple lumped or "distributed-lumped" models are less effective for interconnection delay estimation as operating frequencies approach

*This work was supported by NSF Young Investigator Award MIP-9257982. The work of ABK was supported in part by NSF MIP-9117328 during a Spring 1993 sabbatical visit to UC Berkeley.

the order of GHz (a good review of lumped and distributed RC models is given in [Kum80]). There are also numerous analytical methods for approximating the voltage response of a single distributed line, as reviewed in [ZPK91], but these methods do not easily extend to the delay analysis of arbitrary networks or even tree topologies.

Of particular interest is the class of *moment matching* approaches, which provide acceptable accuracy without sacrificing computational efficiency. Examples of this approach include:

- Horowitz [Hor84] proposed a method for estimating the delay through RC trees using both single-pole and two-pole methods: he calculates the poles of the estimated system response from the first and second moments of the main path (i.e., the unique path from the input node to the output node) in the RC tree. His paper with Rubinstein et al. [RPH83] points out that for delay analysis of RC trees, each distributed RC line should be replaced by a finite number of lumped RC segments to achieve the required accuracy.

- Zhou et al. [ZSTGC92] considered the polynomial describing the poles of a distributed transmission line that is modeled as a single RLC segment driving a small capacitive load.[1] Based on this model, the voltage response in a general interconnection tree is computed from the two dominant poles. To achieve improved accuracy, the authors of [ZSTGC92] propose modeling each tree branch by many shorter segments (but this deviates from the underlying assumptions in that not every branch of the tree drives the small capacitive load).

- McCormick [McC89] also proposed a general technique for approximating the time-domain response of a system from its moment representation, using basic waveforms which are linear, exponentially decaying, underdamped decaying, etc. This method of obtaining waveforms whose moments match those of interest can be used instead of the more traditional two-pole techniques in [Hor84] [ZTG93].

From the recent literature it is clear that moment-matching methods have become increasingly attractive due to their combined efficiency and accuracy. For example, the simulator of Zhou et al. [ZSTGC92] is characterized by its authors as giving delay estimates within several percent of

[1] This model was proposed in [ZPK91]; it assumes that the input to the transmission line has linear $I - V$ characteristics and uses a single RLC segment to model the distributed transmission line.

SPICE; this simulator has been widely distributed, and was used for delay simulations in recent works such as [BKR93] [CLZ93].

The motivation for our present work is simple: the accuracy of any moment-based method depends upon the accuracy of the moment computation itself. For simulation of interconnect trees existing moment-based methods use "distributed-lumped" – i.e., uniformly segmented – representations (e.g., **L**, **T** or **Π** circuits). (For example, both Horowitz and Zhou et al. use **L** segments to model each branch of the interconnect tree.) For such *uniform* representations, one can show that the moments are perfectly captured *only* as the number of segments used approaches infinity, which is computationally unreasonable. When only a finite number of segments are used, the moments will be either underestimated or overestimated depending on the type of segment (**T**, **Π** or **L**). Beyond the need to use only a finite number of segments, other inaccuracies may stem from the underlying analysis itself: for example, Zhou et al. [ZSTGC92] analyze the step response, but use a somewhat incompatible underlying model [ZPK91] for the $I - V$ characteristics. Moreover, it is clearly impossible to obtain the correct first and second moments for a tree when only the polynomial describing the poles of a single *RLC* segment is used (see the discussion below). Thus, the response calculated by [ZSTGC92] is highly approximated; it moreover becomes somewhat impractical when used for trees with long wire segments (e.g., on an MCM substrate, where the *RLC* lossy transmission line model is particularly relevant).

In this paper, we develop very accurate *non-uniform* equivalent circuits for both the distributed *RC* and the distributed *RLC* transmission line models. This concept is originally due to Rajput [Raj74], who proposed an equivalent circuit model with two **L** segments to approximate the response of a distributed *RC* line. The response of Rajput's equivalent circuit was found to be within 3% of the correct distributed response for a step input. Moreover, his equivalent circuit exactly matches the first and second moments of the distributed *RC* line, i.e., the transfer function exactly matches that of the distributed *RC* line up to the coefficient of s^2 in the transfer function. Clearly, this is very desirable in a moment-matching methodology. Furthermore, a computational win arises in that two *non-uniform* **L** segments achieve the exact accuracy that would require an infinite number of *uniform* **L** segments. Sakurai [Sak83] has observed that the use of such an equivalent circuit is not always appropriate, since it cannot predict the correct response when the line is driven bidirectionally. However, in most routing tree design problems,

the source and sinks are fixed and the direction of signal flow is known.

In the following, we present new non-uniform three-segment models which are highly accurate up to the third moment for both the distributed *RC* and the distributed *RLC* transmission line models. We find that our non-uniform three-segment models essentially match exactly the corresponding distributed transfer functions. To evaluate the effect of our equivalent circuits in the context of previous moment-based methods, we use the simple two-pole method and obtain the voltage response for a small tree network studied in [ZSTGC92]. We find that the previous "two-pole" delay estimates of [ZSTGC92] have over 18% error for this instance. Our new non-uniform equivalent circuits can also be employed in place of the lumped T and Π models that are traditionally used for clock skew minimization [Eda93] and other routing applications. For moment-matching approaches, our equivalent circuits use only two or three non-uniform *RLC* segments to achieve the same accuracy as a very large number of uniform segments; this results in very substantial complexity savings. Moreover, the improved accuracy afforded by our results is of particular significance in the design of high-speed systems.

The remainder of this paper is organized as follows. In Section 2, we define the moments of a system and express them using the coefficients of the s terms in the system transfer function. Section 3 then discusses various uniform segmented models used for approximating the response of a distributed transmission line. In Section 4, we develop non-uniform segmented models which accurately capture the moments of the distributed *RC* and *RLC* models; Section 5 compares the uniform and non-uniform models for a simple tree example. Finally, Section 6 compares our methodology with the previous two-pole method of Zhou et al. [ZSTGC92].

2 Moment Representation of the System Transfer Function

The relationships among the moment representation, the Laplace transform of the response, and the time-domain of response are very well discussed in [McC89].

In a linear system the transfer function $H(s) = \frac{V_{out}(s)}{V_{in}(s)}$ gives the relationship between the output response $V_{out}(s)$ and the input response $V_{in}(s)$.

The system transfer function $H(s)$ is related to the impulse response $h(t)$ by the equation

$$H(s) = \int_0^\infty e^{-st} h(t) dt$$

Without loss of generality, the transfer function for any linear system can be expressed as a ratio of polynomials in s, that is to say,

$$H(s) = K \frac{1 + a_1 s + a_2 s^2 + a_3 s^3 + ...}{1 + b_1 s + b_2 s^2 + b_3 s^3 + ...} \tag{1}$$

where K is the DC (zero frequency) gain.

The i^{th} moment of the linear system is defined as

$$M_i = \frac{1}{i!} \int_0^\infty t^i h(t) dt = \frac{(-1)^i}{i!} H^{(i)}(0) \tag{2}$$

where $H^{(i)}(0)$ is the i^{th} derivative of $H(s)$ at $s = 0$.

Assuming $V_{out}(0) = 0$, the Laplace transform of the derivative of the output voltage response for a unit step input is $v'_{out}(t) \Leftrightarrow sV_{out}(s) = s \cdot \frac{1}{s} H(s) = H(s) \Leftrightarrow h(t)$. Therefore, the transfer function can also be written as

$$H(s) = \int_0^\infty e^{-st} v'_{out}(t) dt$$

Expanding e^{-st} into a Maclaurin series,

$$H(s) = \int_0^\infty v'_{out}(t) dt - \frac{s}{1!} \int_0^\infty t v'_{out}(t) dt + \frac{s^2}{2!} \int_0^\infty t^2 v'_{out}(t) dt - \frac{s^3}{3!} \int_0^\infty t^3 v'_{out}(t) dt + \ldots$$

By identifying the integral quantities as moments M_0, M_1, M_2, M_3 etc. from Equation (2),

$$H(s) = (M_0 - sM_1 + s^2 M_2 - s^3 M_3 + ...) \tag{3}$$

Therefore moments can also be defined as

$$M_i = \frac{1}{i!} \int_0^\infty t^i v'_{out}(t) dt \tag{4}$$

We see that the moments of any system can be calculated using the definitions given in Equation (2) or in Equation (3), or by comparing with Equation (4).

Before going further, we note that the Elmore delay, which is defined to be the first moment (M_1) of the system impulse response (i.e., the coefficient of s in the system transfer function

$H(s)$), has received a great deal of attention in the literature. Note that Elmore delay is a first-order approximation and corresponds to a single dominant pole approximation of the response. However, many routing tree techniques [BKR93], [CLZ93] are based on the Elmore delay model. It is well known that Elmore delay is a good analytical representation of delay, but it does not afford any measure of delay with respect to a given threshold voltage [RPH83]. Methods which calculate more than one dominant pole from the moments of the system, e.g., [ZTG93] [Hor84], will lead to a second- or higher-order approximation with improved delay estimates.

The System of Interest: Distributed *RLC* or *RC* Transmission Line

Clearly for any *RLC* network the coefficients a_i and b_i of the transfer function are in terms of the R, L, C circuit parameters (see Appendix A). In Appendix B, we show the relationship between moments and the coefficients a_i and b_i. Here, we seek simple equivalent circuits for the widely studied case of the open-ended distributed transmission line.

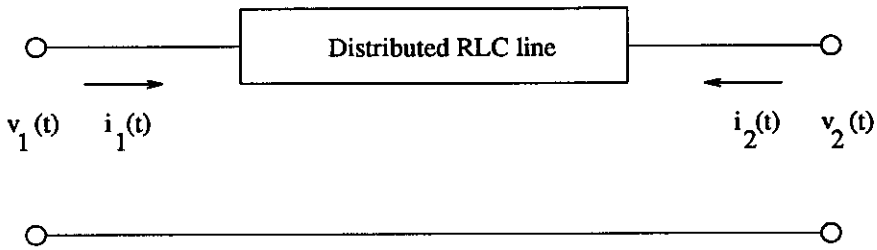

Figure 1: 2-port model of a distributed *RLC* line.

The *ABCD* parameters of a distributed *RLC* transmission line (Figure 1), are [Dwo79]:

$$\begin{pmatrix} V_1(s) \\ I_1(s) \end{pmatrix} = \begin{pmatrix} cosh(\theta h) & Z_0 sinh(\theta h) \\ \frac{1}{Z_0} sinh(\theta h) & cosh(\theta h) \end{pmatrix} \begin{pmatrix} V_2(s) \\ I_2(s) \end{pmatrix} \tag{5}$$

where $\theta = \sqrt{(r + sl)sc}$, h = length of the line and $r = \frac{R}{h}$, $l = \frac{L}{h}$ and $c = \frac{C}{h}$ are the resistance, inductance and capacitance per unit length.

Since $I_2(s) = 0$ for an open-ended distributed *RLC* line the voltage response at the end of the line is

$$V_2(s) = \frac{V_1(s)}{\cosh(\theta h)} \quad .$$

Therefore, the numerator polynomial of the open-ended transfer function for distributed *RLC*

Coefficients	Distributed Line Model	
	RLC	RC
b_1	$\frac{RC}{2} = 0.50RC$	$\frac{RC}{2} = 0.50RC$
b_2	$\frac{(RC)^2}{24} + \frac{LC}{2} = 0.0417(RC)^2 + 0.50LC$	$\frac{(RC)^2}{24} = 0.0417(RC)^2$
b_3	$\frac{(RC)^3}{720} + \frac{RLC^2}{12} = 0.0014(RC)^3 + 0.0833RLC^2$	$\frac{(RC)^3}{720} = 0.0014(RC)^3$

Table 1: Coefficients of s's for both distributed RLC and RC models.

line is just a constant (i.e., all a's = 0) and is given by

$$\begin{aligned} H(s) &= \frac{1}{\cosh(\sqrt{(R+sL)sC})} \\ &= \frac{1}{1 + \frac{(R+sL)sC}{2!} + \frac{(R+sL)^2(sC)^2}{4!} + \frac{(R+sL)^3(sC)^3}{6!} + \ldots} \\ &= \frac{1}{1 + \frac{RC}{2}s + (\frac{(RC)^2}{24} + \frac{LC}{2})s^2 + (\frac{(RC)^3}{720} + \frac{RLC^2}{12})s^3 + \ldots} \end{aligned} \quad (6)$$

The coefficients of s's for a distributed RLC line are tabulated in Table 1. The analogous coefficients for the case of a distributed RC line are obtained by substituting $L = 0$ in Equation (6).

3 Uniform Segment Models

We now discuss the open-ended transfer functions for various lumped models such as **L**, **T** or **Π** models, which have traditionally been used to approximate the behavior of the distributed transmission line. Since the analyses for for **T** and **Π** are very similar, we will discuss only the case of **T** circuits.

3.1 Uniform L Segments

The open-ended transfer function for two uniform **L** segments (Figure 2) is

$$H_{2L}(s) = \frac{1}{1 + s(R_1(C_1 + C_2) + R_2C_2) + s^2R_1R_2C_1C_2}$$

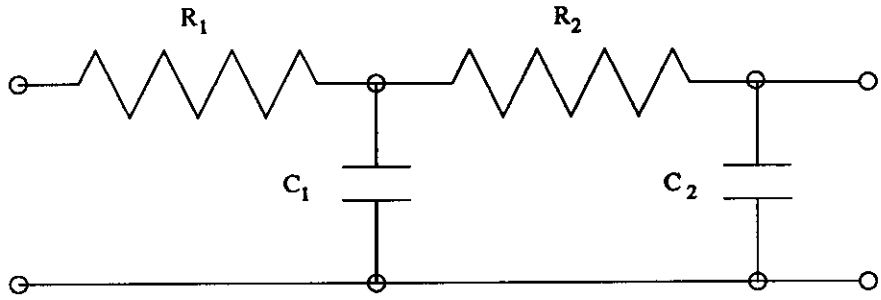

Figure 2: A distributed RC line modeled using two uniform **L** segments.

When resistance and capacitance values are uniformly divided between the segments, we substitute $R_1 = R_2 = R/2$ and $C_1 = C_2 = C/2$ into the above equation and find

$$H_{2L}(s) = \frac{1}{1 + \frac{3RC}{4}s + \frac{(RC)^2}{16}s^2} \tag{7}$$

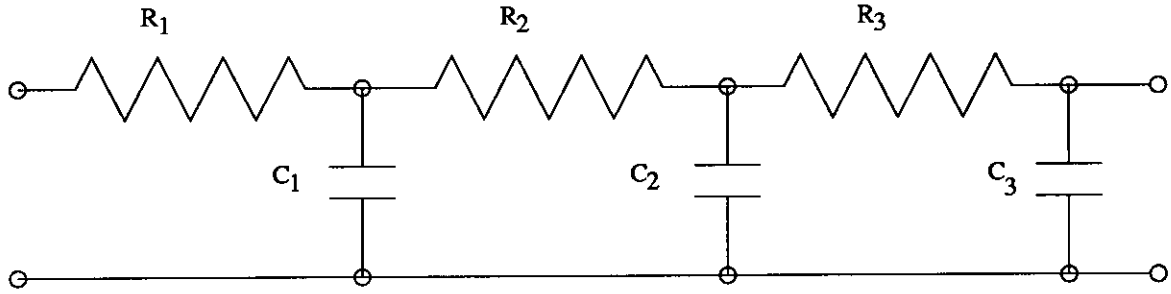

Figure 3: Three **L**-type RC segment model for a distributed RC line.

Similarly, the open-ended transfer function for three uniform **L** segments (Figure 3) is

$$H_{3L}(s) = \frac{1}{1 + sb_1 + s^2b_2 + s^3b_3}$$

where

$$b_1 = (R_1(C_1 + C_2 + C_3) + R_2(C_2 + C_3) + R_3C_3)$$

$$b_2 = (R_1R_2C_1C_3 + R_1R_3C_1C_3 + R_2R_3C_2C_3 + R_1R_3C_2C_3 + R_1R_2C_1C_3)$$

$$b_3 = R_1R_2R_3C_1C_2C_3$$

Substituting $R_1 = R_2 = R_3 = R/3$ and $C_1 = C_2 = C_3 = C/3$ into the above equation, we get

$$H_{3L}(s) = \frac{1}{1 + \frac{2RC}{3}s + \frac{5(RC)^2}{81}s^2 + \frac{(RC)^3}{729}s^3} \tag{8}$$

As the number of segments tends to infinity, the **L** type model approaches the RC distributed line model given in Equation (6) with $L = 0$. We have proved that as $N \to \infty$, b_1, b_2 and b_3 all tend to their respective values given in Equation (6) (details are given in Appendix C).

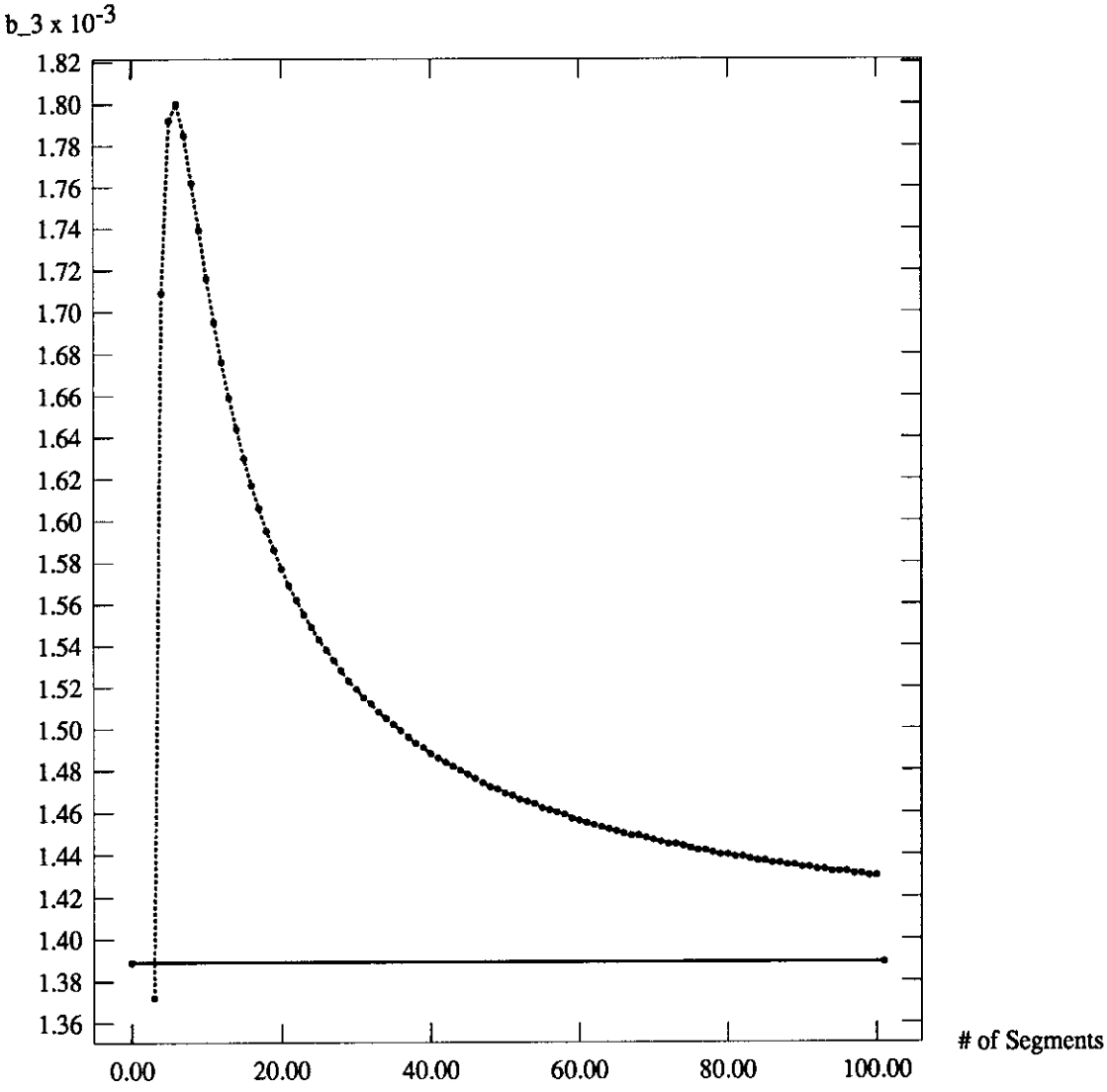

Figure 4: Convergence of b_3 (the coefficient of s^3) with respect to uniform **L** segments. The correct value of b_3 is $1/720 = 1.39X10^{-3}$.

The convergence of b_3 is plotted for different numbers of uniform segments, Figure 4. Interestingly, b_3 is not monotone with respect to the number of segments. From the Figure, we see that the coefficient b_3 is close to its optimal value of $1/720$ when there three uniform segments, but then increases to its maximum error (seven uniform segments) before decreasing. For example,

using 10 uniform segments to approximate the behavior of a distributed RLC line entails error in the coefficient b_3 of around 25%. At the same time, the error in b_1 is around 10% and that of b_2 is 20%, also for the 10 uniform segment approximation. The corresponding errors in the first moment and second moment are 10% and 20%, respectively. Since the voltage response is exponentially dependent on these moments, the resultant error in the response can be quite high. As we show below, it is always better to use **non-uniform** segments which can more accurately approximate the transfer function of the distributed line.

3.2 Uniform T Segments

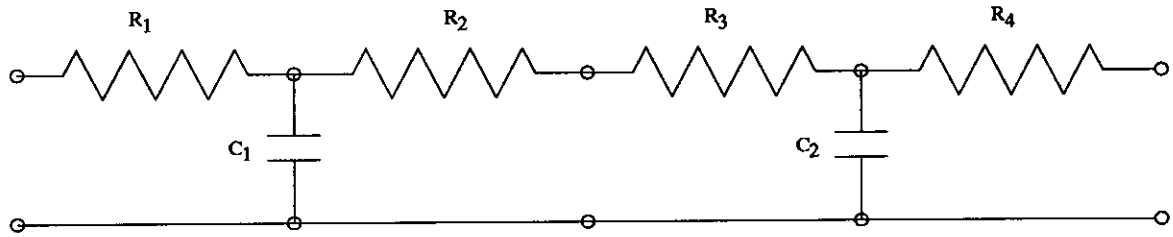

Figure 5: Two uniform **T** segments model for a distributed RC line.

The open-ended transfer function for two uniform **T** segments (Figure 5) is

$$H_{2T}(s) = \frac{1}{1 + s(R_1(C_1 + C_2) + (R_2 + R_3)C_2) + s^2 R_1(R_2 + R_3)C_1C_2} \tag{9}$$

Substituting the uniformly distributed resistance and capacitance values $R_1 = R_2 = R_3 = R_4 = R/4$ and $C_1 = C_2 = C/2$ into the above equation yields

$$H_{2T}(s) = \frac{1}{1 + \frac{RC}{2}s + \frac{(RC)^2}{32}s^2} \tag{10}$$

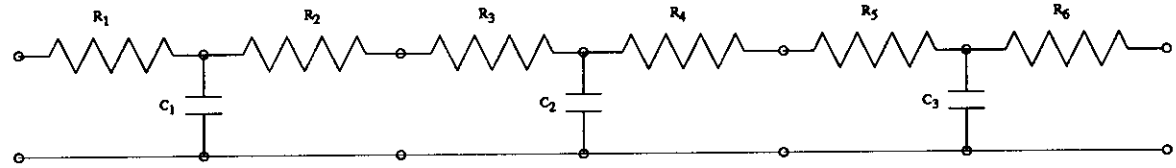

Figure 6: 3 T segments model for a distributed RC line.

Similarly, the open-ended transfer function for three uniform **T** segments is (Figure 6) is,

$$H_{3T}(s) = \frac{1}{1 + b_1 s + b_2 s^2 + b_3 s^3} \tag{11}$$

where

$$b_1 = R_1(C_1 + C_2 + C_3) + (R_2 + R_3)(C_1 + C_2) + (R_4 + R_5)C_3$$

$$b_2 = (R_1(R_2+R_3)C_1C_3+R_1(R_4+R_5)C_1C_3+(R_2+R_3)(R_4+R_5)C_2C_3+R_1(R_4+R_5)C_2C_3+R_1(R_2+R_3)C_1C_3)$$

$$b_3 = R_1(R_2 + R_3)(R_4 + R_5)C_1C_2C_3$$

Substituting the uniformly distributed resistance and capacitance values $R_1 = R_2 = R_3 = R_4 = R_5 = R_6 = R/6$ and $C_1 = C_2 = C_3 = C/3$ into the above equation yields

$$H_{3T}(s) = \frac{1}{1 + \frac{RC}{2}s + \frac{(RC)^2}{27}s^2 + \frac{(RC)^3}{1458}s^3} \tag{12}$$

Sakurai [Sak83] showed that for both the **T** and Π models, the open-ended transfer function also converges to the distributed RC transfer function as the number of segments tend to infinity, i.e., all the moments will converge to their respective values given in Equation (6). A comparison of various lumped models approximating the distributed RC line is given in Table 2. It is clear that for any finite number of segments the uniform T segments **underestimate** the coefficient of s^2, while the uniform **L** segments **overestimate** the coefficients of s and s^2 in the denominator of the transfer function. While we have only presented the analysis of various lumped RC models, we have also extended our study to lumped RLC models; this analysis is summarized in Table 3.

4 Non-Uniform Segment Models

Rajput [Raj74] proposed the following equivalent circuit, composed of two non-uniform **L** segments, for a distributed RC line. The circuit element values (refer to Figure 2) are given by

$$R_1 = \frac{1}{4}R, \qquad R_2 = \frac{3}{4}R$$

$$C_1 = \frac{2}{3}C, \qquad C_2 = \frac{1}{3}C$$

and the open-ended transfer function for this equivalent circuit is given by

$$H_{Raj_2}(s) = \frac{1}{1 + \frac{RC}{2}s + \frac{(RC)^2}{24}s^2} \tag{13}$$

Thus, the open-ended transfer function of a distributed RC line (Equation (6)) is captured **exactly** up to the coefficient of s^2, i.e., the first and second moments are exactly the same as for the distributed RC line. From the convergence analysis of b_1, b_2, b_3 in Appendix C, we know that uniform segments can achieve this accuracy only as the number of segments tends to infinity ($N \rightarrow \infty$). Since the accuracy of the two-pole method [ZTG93] [ZSTGC92] depends on the first and second moments, use of this non-uniform equivalent circuit to model the interconnect lines in tree networks will lead to improved delay estimates. In this section, we will calculate non-uniform equivalent circuits to estimate the higher moments and also extend the technique to RLC models.

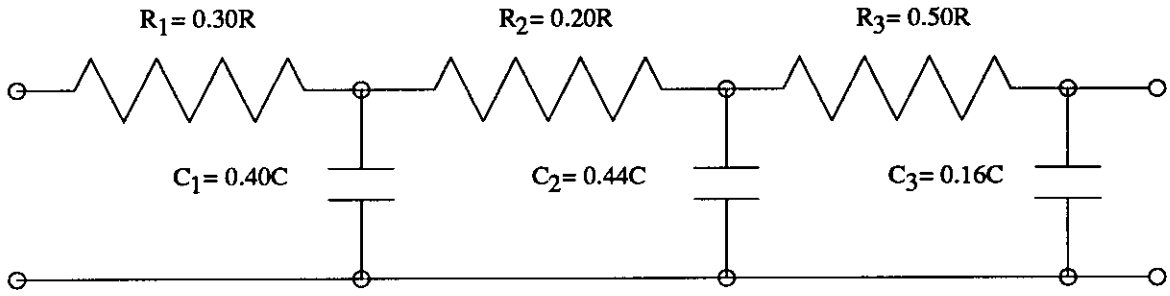

Figure 7: Non-uniform three **L** segment model for a distributed RC line.

4.1 RC Segment Model

For three non-uniform **L** type RC segments as shown in (Figure 7), we solve for the values of the resistances and capacitances by calculating the open-ended transfer function and the open-circuit input impedance; this leads to 7 equations with 6 unknowns, an overspecified system (see Appendix E). Since there are no solutions to this system of equations, we have used numerical techniques to minimize the squared error in the b_1, b_2 and b_3 values. We thus obtained the following circuit parameters:

$$R_1 = 0.30R, \quad R_2 = 0.20R, \quad R_3 = 0.50R$$

$$C_1 = 0.40C, \quad C_2 = 0.44C, \quad C_3 = 0.16C$$

The corresponding coefficients of s's in the transfer function are

$$b_1 = 0.50RC, \quad b_2 = 0.0416(RC)^2, \quad b_3 = 0.0009(RC)^3$$

These values are extremely close to the exact values given in Equation (6), and we can improve the accuracy of coefficients of s's by extending the precision to which we express the circuit parameters. The contrast between non-uniform and various uniform RC models used for approximating the behavior of the transmission line is also shown in Table 2.

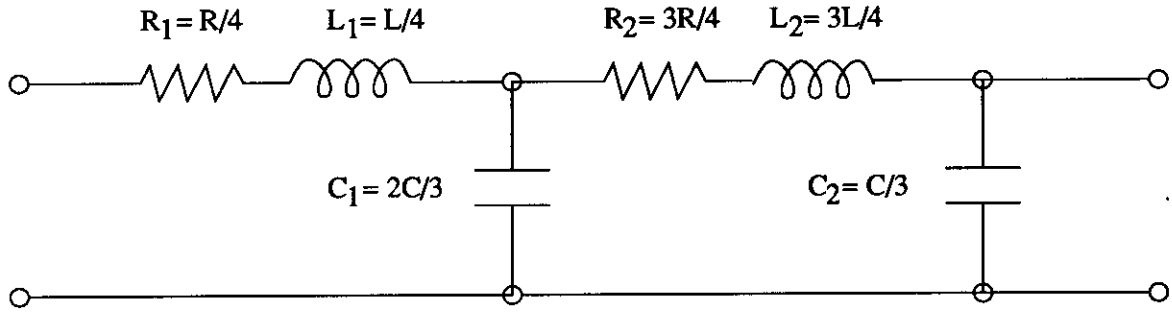

Figure 8: Non-uniform two **L** segments model for a distributed RLC line.

4.2 RLC Segment Models

Extending the equivalent-circuit technique to an RLC model is straightforward (see Appendix E). For two non-uniform RLC segments (Figure 8), we obtain the following values for the circuit components:

$$R_1 = \frac{1}{4}R, \qquad R_2 = \frac{3}{4}R$$
$$L_1 = \frac{1}{4}L, \qquad L_2 = \frac{3}{4}L$$
$$C_1 = \frac{2}{3}C, \qquad C_2 = \frac{1}{3}C$$

for which the corresponding coefficients of s's are

$$b_1 = \frac{1}{2}RC$$
$$b_2 = \frac{1}{24}(RC)^2 + \frac{1}{2}LC$$
$$b_3 = \frac{1}{12}RLC^2$$

In other word, the open-ended transfer function for these two non-uniform RLC segments is

$$H(s) = \frac{1}{1 + \frac{RC}{2}s + (\frac{(RC)^2}{24} + \frac{LC}{2})s^2 + \frac{RLC^2}{12}s^3} \tag{14}$$

By comparing Equation (14) with Equation (6), we see that two non-uniform RLC segments can obtain the first and second moments exactly. Notice the similarity of the inductance values

to the corresponding resistance values. We offer the conjecture that in any optimal non-uniform RLC equivalent circuit the distributions of the resistance and inductance should be the same.

We have also numerically optimized the equivalent circuit with three non-uniform RLC segments. The optimized circuit elements are

$$R_1 = 0.30R, \quad R_2 = 0.20R, \quad R_3 = 0.50R$$

$$L_1 = 0.30L, \quad L_2 = 0.20L, \quad L_3 = 0.50L$$

$$C_1 = 0.40C, \quad C_2 = 0.44C, \quad C_3 = 0.16C$$

which imply the following coefficients in the transfer function:

$$b_1 = 0.50RC$$

$$b_2 = 0.0416(RC)^2 + 0.50LC$$

$$b_3 = 0.0009(RC)^3 + 0.832RLC^2$$

Therefore, the open-ended transfer function for the three non-uniform RLC segment model is

$$H(s) = \frac{1}{1 + \frac{RC}{2}s + (\frac{(RC)^2}{24} + \frac{LC}{2})s^2 + (\frac{(RC)^3}{1111.11} + \frac{RLC^2}{12.02})s^3} \tag{15}$$

Our non-uniform three-segment RLC model obtains the first and second moments exactly, and the third moment almost exactly. Table 3 provides a comparison of non-uniform and uniform RLC models used to approximate the distributed RLC model of the transmission line. Using these non-uniform equivalent circuits in a higher-order approximation of the transfer function will yield a more accurate voltage response than using any number of uniform segment models (i.e., the approach used in [ZSTGC92]).

4.3 The Complexity Win

For large routing trees, using non-uniform equivalent circuits for a distributed RLC line will reduce the computation time significantly compared to using a number of uniform RLC segments. Recall that previous works suggest using k segments to model each interconnect line (for instance, [CLZ93] divides each line into $25\mu m$ segments and then models each segment using a uniform **L**

Method	b_1	b_2	b_3
Distributed RC Line Model	$\frac{RC}{2}$	$\frac{(RC)^2}{24}$	$\frac{(RC)^3}{720}$
One uniform L segment	RC	0	0
Two uniform L segments	$\frac{3RC}{4}$	$\frac{(RC)^2}{16}$	0
Three uniform L segments	$\frac{2RC}{3}$	$\frac{5(RC)^2}{81}$	$\frac{(RC)^3}{729}$
One uniform T segment	$\frac{RC}{2}$	0	0
Two uniform T segments	$\frac{RC}{2}$	$\frac{(RC)^2}{32}$	0
Three uniform T segments	$\frac{RC}{2}$	$\frac{(RC)^2}{27}$	$\frac{(RC)^3}{1458}$
Two non-uniform L segments	$\frac{RC}{2}$	$\frac{(RC)^2}{24}$	0
Three non-uniform L segments*	$\frac{RC}{2}$	$\frac{(RC)^2}{24.04}$	$\frac{(RC)^3}{1111.11}$

Table 2: Various models approximating the open-ended transfer function of distributed RC line.* These values are computed numercially, since the corresponding system of equations is overspecified.

type RLC circuit), and for MCM interconnects k can be very large. Let N be the total number of interconnect lines from the input node to the output node (i.e., on the main path). From the expressions given in Appendix A, the computation time of b_1 is $O\left((kN)^2\right)$, that of b_2 is $O\left((kN)^4\right)$ and that of b_3 is $O\left((kN)^6\right)$. Using two non-uniform segments the computation time will be reduced to $O(N^2)$ for b_1, $O(N^4)$ for b_2 and $O(N^6)$ for b_3, which will be a very significant reduction if the interconnection tree is large or if accuracy is desired. As we pointed out earlier, to achieve the accuracy of the non-uniform models, the number of uniform segments required is infinite ($k = \infty$). With 10 uniform segments, the errors in the first and second moments are 10% and 20%; even with 25 uniform segments these errors are still 5% and 8%.

5 Sample Analysis: A Small Tree Circuit

Method	b_1	b_2	b_3
Distributed RLC Line Model	$\frac{RC}{2}$	$\frac{(RC)^2}{24} + \frac{LC}{2}$	$\frac{(RC)^3}{720} + \frac{RLC^2}{12}$
Two uniform L segments	$\frac{3RC}{4}$	$\frac{(RC)^2}{16} + \frac{3LC}{4}$	$0 + \frac{RLC^2}{8}$
Three uniform L segments	$\frac{2RC}{3}$	$\frac{5(RC)^2}{81} + \frac{LC}{2}$	$\frac{(RC)^3}{729} + \frac{10RLC^2}{81}$
Two uniform T segments	$\frac{RC}{2}$	$\frac{(RC)^2}{32} + \frac{LC}{2}$	$0 + \frac{RLC^2}{16}$
Three uniform T segments	$\frac{RC}{2}$	$\frac{(RC)^2}{27} + \frac{LC}{2}$	$\frac{(RC)^3}{1458} + \frac{2RLC^2}{27}$
Two non-uniform L segments	$\frac{RC}{2}$	$\frac{(RC)^2}{24} + \frac{LC}{2}$	$0 + \frac{RLC^2}{12}$
Three non-uniform L segments	$\frac{RC}{2}$	$\frac{(RC)^2}{24} + \frac{LC}{2}$	$\frac{(RC)^3}{1111.11} + \frac{RLC^2}{12.02}$

Table 3: Various models approximating the open-ended transfer function of distributed RLC line.

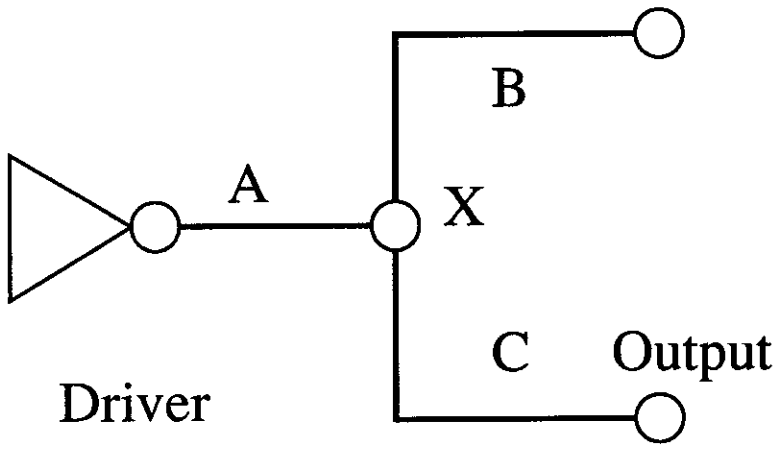

Figure 9: A simple tree with three transmission lines.

To show the practical impact of the non-uniform equivalent circuit, we now show the inaccuracy of uniform segment models when applied to the small tree shown in Figure 9. For the tree analysis we use the same approach as [ZSTGC92], which identifies the main path between the input node and the output node and then replaces all off-path branches by their respective capacitive impedances. The simple tree we consider has three transmission lines A, B and C; the driver is connected to the front of line A and the output node is at the end of line C. Therefore, line B is

an off-path branch and will be replaced by an equivalent capacitive load at the intersection point X.

Case 1: One Uniform **L** Segment. Replacing each tree branch by one RC segment and the off-path branch by its capacitive impedance, we obtain the following the transfer function for the main path:

$$H(s) = \frac{1}{1 + s(R_A C_A + R_A C_B + R_A C_C + R_C C_C) + s^2 R_A R_C (C_A + C_B) C_C} \tag{16}$$

Case 2: Two Uniform **L** Segments. Using two uniform **L** segments to model each tree branch, the transfer function of the main path is:

$$H(s) = \frac{1}{1 + b_1 s + b_2 s^2 + ...} \tag{17}$$

where

$$\begin{aligned} b_1 &= \frac{3}{4} R_A C_A + R_A C_B + R_A C_C + \frac{3}{4} R_C C_C \\ b_2 &= \frac{(R_A C_A)^2}{16} + \frac{R_A^2 C_A C_B}{8} + \frac{9 R_A R_C C_A C_C}{16} + \frac{3 R_A R_C C_B C_C}{4} + \frac{(R_C C_C)^2}{8} \\ &\quad + \frac{R_A R_C C_C^2}{16} + \frac{R_A^2 C_A C_C}{8} \end{aligned}$$

Case 3: One Uniform **T** Segment. Replacing each tree branch by one **T** segment, the transfer function for the main path is

$$H(s) = \frac{1}{1 + b_1 s + b_2 s^2 + b_3 s^3} \tag{18}$$

where

$$\begin{aligned} b_1 &= \frac{1}{2} R_A C_A + R_A C_B + R_A C_C + \frac{1}{2} R_C C_C \\ b_2 &= \frac{R_A^2 C_A C_B}{4} + \frac{R_A R_C C_A C_C}{4} + \frac{R_A R_C C_B C_C}{2} + \frac{R_A^2 C_A C_C}{4} \\ b_3 &= \frac{R_A R_C C_A C_B C_C}{8} \end{aligned}$$

Case 4: Non-uniform Two **L** Segments. Using the two non-uniform RC segment model for each tree branch, the transfer function of the main path is

$$H(s) = \frac{1}{1 + b_1 s + b_2 s^2 + ...} \tag{19}$$

where

$$\begin{aligned} b_1 &= \frac{1}{2}R_A C_A + R_A C_B + R_A C_C + \frac{1}{2}R_C C_C \\ b_2 &= \frac{(R_A C_A)^2}{24} + \frac{R_A^2 C_A C_B}{8} + \frac{R_A R_C C_A C_C}{4} + \frac{R_A R_C C_B C_C}{2} + \frac{(R_C C_C)^2}{24} \\ &\quad + \frac{R_A R_C C_C^2}{6} + \frac{R_A^2 C_A C_C}{8} \end{aligned}$$

From the transfer function of a distributed RLC line given in Equation (6), we know that the effect of the branch **A** should be $\frac{R_A C_A}{2}$ in the coefficient of s, i.e., in b_1, and the effect on b_2 should be $\frac{(R_A C_A)^2}{24}$. By comparing Equations (16) - (19), we see that the coefficient of s is correct only in **Case 3** (one uniform **T** segment) and **Case 4** (two non-uniform segments). The coefficient of s^2 is correct only in **Case 4**. Again, note that all previous approaches based on pole calculations use uniform **L**, **T** or **Π** equivalent circuits in the delay calculation.

6 Experimental Results: Two-Pole Method for Tree Analysis

In this section, we give a stronger demonstration of the effect of equivalent circuit models, by considering the "two-pole" simulation methodology. Zhou et al. [ZPK91] proposed an analytical approach for calculating the dominant poles for a single transmission line by using a single RLC segment as the underlying model. In their analysis, they assume a linear model for the sources $I - V$ curve and obtain a polynomial describing the poles of the transmission line. By making various assumptions about this polynomial, they obtain the poles of interest ([ZPK91], p. 781). Based on this work, Zhou et al. [ZSTGC92] then compute poles of a tree of general RLC interconnection segments. Since the polynomial obtained in [ZPK91] is based on a single RLC segment, the coefficient of s^2 (i.e., b_2) will not have any $(RC)^2$ term. Thus, order to improve the accuracy, [ZSTGC92]) use multiple RLC segments to model each distributed line. The polynomial used in their calculations is given by ([ZSTGC92], p.11):

$$\left(\frac{LC}{2} + LC_g\right)s^2 + \left(\frac{RC}{2} + RC_g + R_0(C + C_g)\right) + \gamma_m = 0 \tag{20}$$

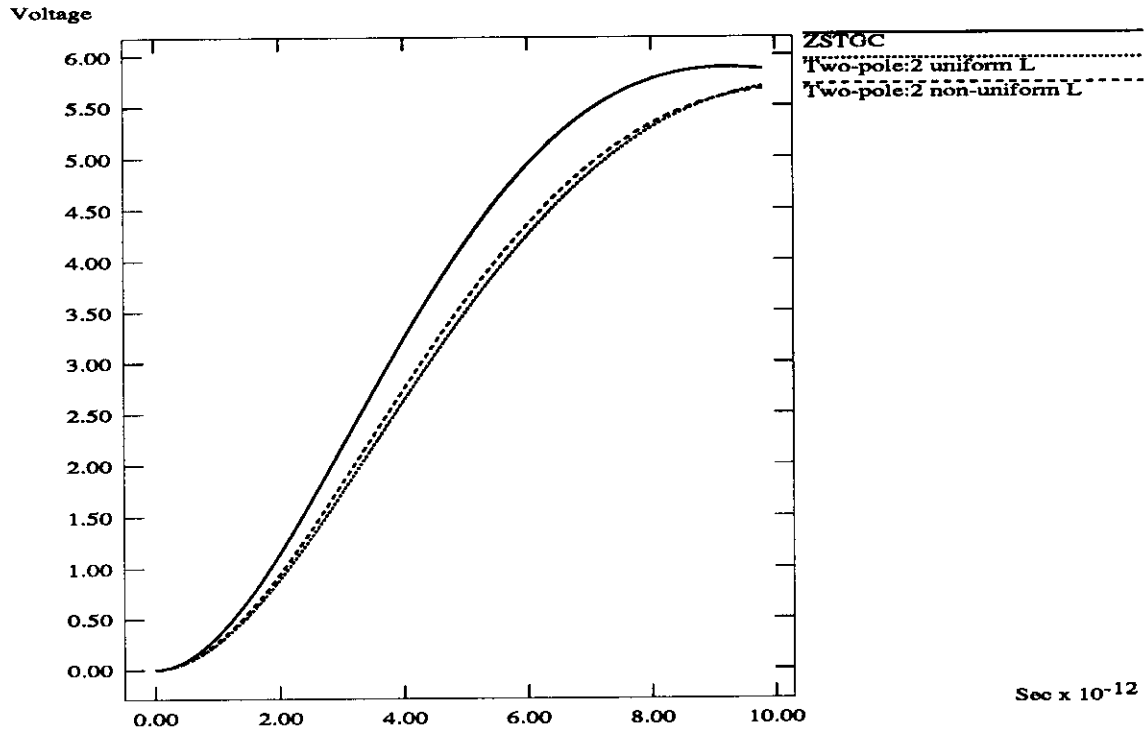

Figure 10: Unit step response at node 6 of the tree shown in Figure 10, using both uniform and non-uniform models and the two-pole approximation. Here, driver resistance is 10Ω. ZSTGC is the previous approximate method of [ZSTGC92], and "Two-Pole" is the standard method discussed in the standard method proposed in [Hor84] [ZTG93].

which can be expressed in the form

$$\tau_2 s^2 + \tau_1 s + \gamma_m = 0$$

For the tree analysis, the first and second moments are computed as described in Appendix B, and then matched as first moment for τ_1, and second moment for τ_2. There is no clear relationship between the first and second moments and the τ_1 and τ_2 values, except for the case of a *single* transmission line.

Here, we calculate the voltage response for interconnection trees with the non-uniform segment model, using the standard two-pole approximation for the system transfer function developed by [Hor84] [ZTG93]. The system transfer function in terms of the poles is approximated by

$$H(s) = \frac{k_1}{s - s_1} + \frac{k_2}{s - s_2}$$

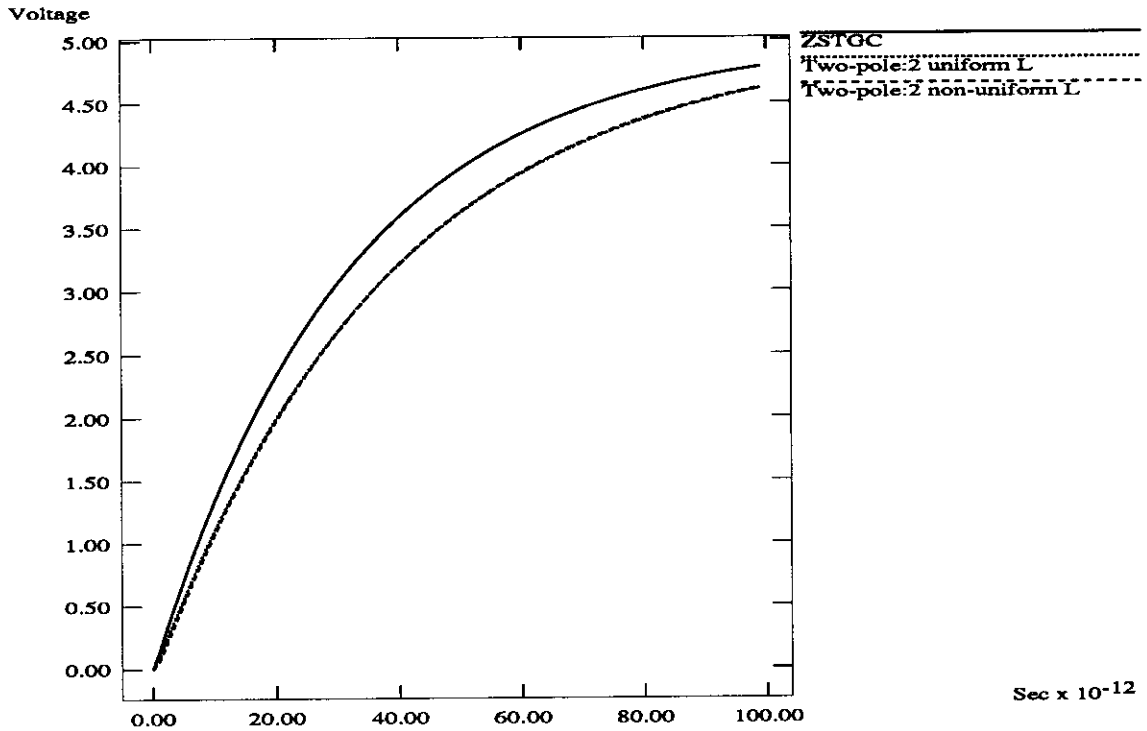

Figure 11: Unit step response at node 6 of the tree shown in Figure 10, using both uniform and non-uniform models and the two-pole approximation. Here, driver resistance is 150Ω.

where s_1, s_2 are the poles and k_1, k_2 are the coefficients corresponding to the poles. (Appendix D describes the poles and coefficients in terms of the moments and also gives the expression for voltage response.) For the tree analysis, we first identify the main path from the source to the output node and then replace all off-path subtrees by their respective capacitive loads [ZSTGC92]. The delay computed in this way is clearly an upper bound on the exact delay. Using this two-pole methodology we compared the non-uniform and uniform segment models. We plotted the voltage response at Node 6 of the tree interconnection layout studied in [ZSTGC92] (Figure 12), for different models and using different driver resistances. Note that in [ZSTGC92], they calculate the response assuming a driver resistance of 10Ω. (This is perhaps not very realistic: as noted in [ZPK91] [WE88], a more appropriate driver resistance is in the range of $[200\Omega, 4000\Omega]$.) The voltage response for the driver resistance of 10Ω are given in Figure 10. Similarly we plotted the response for a driver resistance of 150Ω (Figure 11). In these plots, the previous delay times for 90% threshold voltage are off by around 14%.

To demonstrate the increase of error for longer interconnects, we used the same tree but

scaled the length of the branches (edges) between nodes (1,2) and between nodes (2,3) by a factor of 10. All other branch lengths were kept the same. The response at Node 6 is given in Figure 13, and the error in the 90% threshold delay between two uniform *RLC* segments and non-uniform *RLC* segments is around 18%. As the driver resistance decreases or as the wire length increases, the difference between these models becomes much more significant. For high-speed systems, or MCM layout applications where the wire lengths become very large, our *non-uniform* segment model will allow improved accuracy and efficiency when compared with previous two-pole methods.

7 Conclusions

For high-speed systems, accurate estimation of the propagation delays due to interconnects is one of the main obstacles for correct system implementation. In this paper, we develop compact, *optimal* equivalent circuits for estimating the delays in single RLC interconnects and interconnect tree topologies. These equivalent circuits are calculated either analytically or else using numerical techniques when the governing system of equations is overspecified. Our non-uniform *RLC* segment models approximate the transfer function of the distributed line very accurately using only two or three segments; moreover, the same technique can be used to derive equivalent circuits for a distributed *RLCG* model of the transmission line.

We give a practical demonstration of our technique's advantages, in the context of the two-pole approximation approach [Hor84] [ZSTGC92] [ZTG93] (which uses the first two moments). Since the first and second moments are matched exactly by our new non-uniform models, we obtain very accurate delay estimates that would be possible only with a very large number of uniform segments. We show that the delay estimates of previous methods [ZSTGC92] are incorrect by anywhere from 14 to 20%, even for a very small routing topology. Such differences are very significant for critical timing analyses in the design of high-speed systems. We believe that the non-uniform equivalent circuits can be useful in place of the lumped T and Π models that are traditionally used for delay estimation, clock skew minimization [Eda93] and other routing applications. Moreover, the evaluations of existing routing tree techniques (such as Elmore routing trees [BKR93] or A-trees [CLZ93]), whose delays were measured using the technique of [ZSTGC92], may change. Finally, there is an obvious complexity reduction since our method

uses only two or three segments instead of many segments.

So far in the analysis, we used only the two dominant poles for the calculation of the voltage response. We can extend the application of our result to obtain a more accurate analysis, by including additional dominant poles and zeros, and also by using a higher-order approximation for the system transfer function. Computation of higher moments (e.g., M_3, M_4, etc.) is required for the analysis of these higher-order transfer functions. As an example, retaining the assumption of two dominant poles with a higher-order system, we would have a transfer function of form $H(s) = \frac{k_1}{(s-s_1)} + \frac{k_2}{(s-s_2)^2}$. For the voltage response calculation of the above system, we need only the first three moments to establish the boundary conditions.

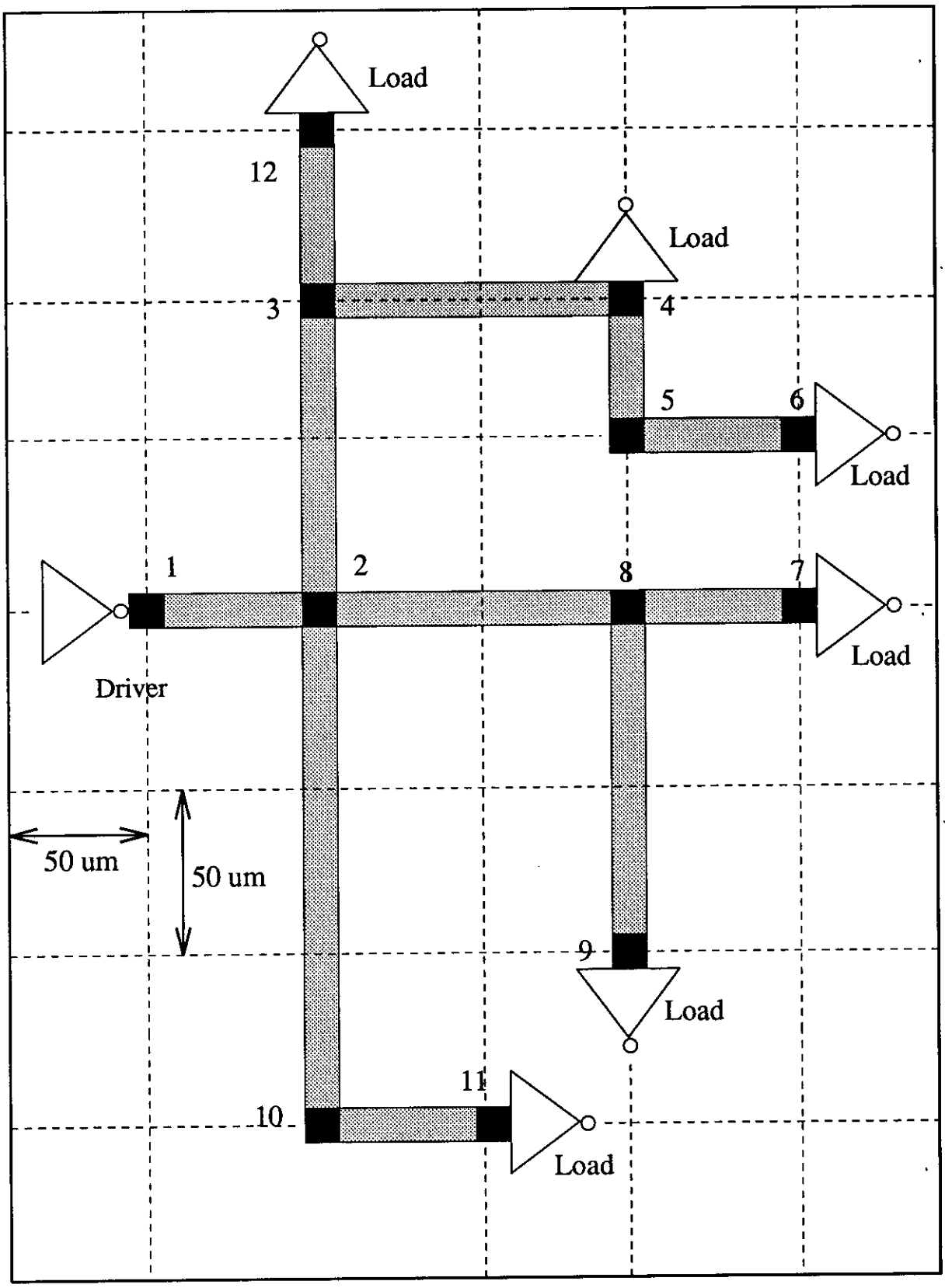

Figure 12: A tree interconnection layout from [ZSTGC92].

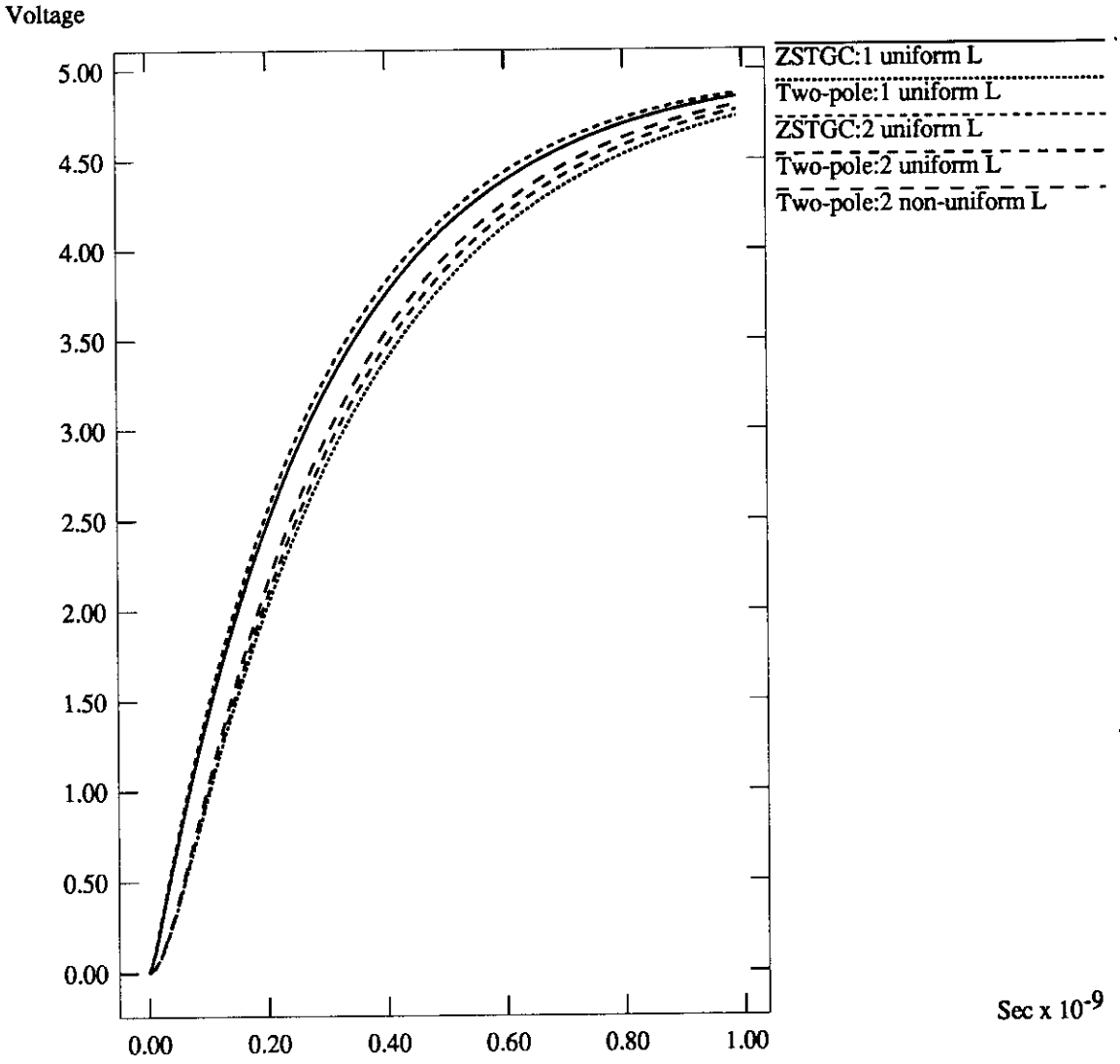

Figure 13: Unit step response at the node 6 in same tree topology as that of Figure 10, with the branches (edges) between nodes $(1,2)$ and between nodes $(2,3)$ scaled by a factor of 10. Again, we compare uniform and non-uniform models using the two-pole approximation; driver resistance is 150Ω.

Appendix A: Calculation of the Coefficients of s Terms in the the Denominator Polynomial of the Transfer Function

In this Appendix, we derive the values of b_1, b_2 and b_3, which are respectively the coefficients of the s, s^2 and s^3 terms in the denominator polynomial of Equation (1), in terms of the R, L, and C circuit parameters. (For the distributed RLC line, all coefficients a_i in the numerator polynomial are identically zero.)

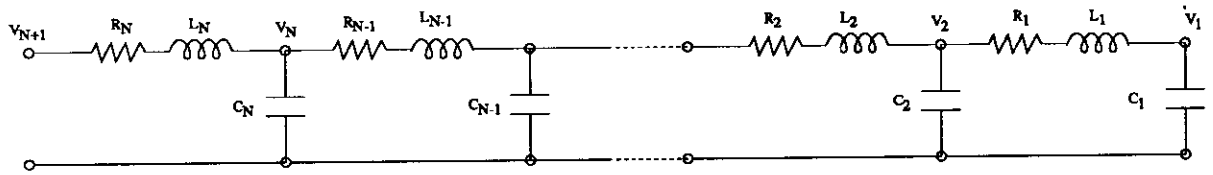

Figure 14: N-segment distributed RLC transmission line model.

Consider a single RLC transmission line that is modeled with N segments. These RLC segments are connected as shown in Figure 14. For this structure, Gao et al. [GZ93] have shown that the input voltage $V_{N+1}(s)$ can be written as

$$V_{N+1}(s) = (R_N + sL_N)\sum_{j=1}^{N} sC_jV_j(s) + V_N(s) \tag{21}$$

Thus, $V_{N+1}(s)$ can be expressed as a series in s, i.e.,

$$\begin{aligned} V_{N+1}(s) &= V_1(s)(1 + \sum_{j=1}^{2N} b_j s^j) \\ &= V_1(s)(1 + b_1 s + b_2 s^2 + b_3 s^3 + ...) \end{aligned} \tag{22}$$

From Equation (21), we see that the coefficient of s in $V_{N+1}(s)$ is given by the coefficient of s in $V_N(s)$, plus R_N times the summation $\sum_{j=1}^{N} C_j \cdot$ (constant terms in $V_j(s)$).

We will use the notation b_1^{N+1} to denote the coefficient of s in $\frac{V_{N+1}(s)}{V_1(s)}$, i.e., the transfer function at node $(N+1)$. Thus, we have

$$b_1^{N+1} = R_N \sum_{j=1}^{N} C_j + b_1^N$$

From Equation (22), we see that b_1^{N+1} is simply b_1. Therefore,

$$b_1 = R_N \sum_{j=1}^{N} C_j + R_{N-1} \sum_{j=1}^{N-1} C_j + ...$$

$$= \sum_{i=1}^{N} R_i \left(\sum_{j=1}^{i} C_j \right)$$

By changing the order of variables in the double summation, we obtain

$$b_1 = \sum_{j=1}^{N} C_j \sum_{i=j}^{N} R_i \tag{23}$$

To obtain an expression for b_2, we return to Equation (21), where we see that the coefficient of s^2 in $V_{N+1}(s)$ can be written as the sum of three terms: (i) the product of R_N times the summation $\sum_{j=1}^{N} C_j$· (coefficient of s in $V_j(s)$); (ii) the product of L_N times the summation $\sum_{j=1}^{N} C_j$ (constant terms in $V_j(s)$); and (iii) the coefficient of s^2 in $V_N(s)$. Using the same notation as above:

$$b_2 = b_2^{N+1} = R_N \sum_{j=1}^{N} C_j b_1^{j-1} + L_N \sum_{j=1}^{N} C_j + b_2^N$$

Therefore,

$$\begin{aligned} b_2 &= [R_N \sum_{j=1}^{N} C_j \left(\sum_{i=1}^{j-1} C_i (\sum_{d=i}^{j-1} R_d) \right) + R_{N-1} \sum_{j=1}^{N-1} C_j \left(\sum_{i=1}^{j-1} C_i (\sum_{d=i}^{j-1} R_d) \right) + ...] \\ &\quad + [L_N \sum_{j=1}^{N} C_j + L_{N-1} \sum_{j=1}^{N-1} C_j + ...] \\ &= [\sum_{l=2}^{N} R_l \left(\sum_{j=1}^{l} C_j \left(\sum_{i=1}^{j-1} C_i (\sum_{d=i}^{j-1} R_d) \right) \right)] + [\sum_{l=1}^{N} L_l \left(\sum_{j=1}^{l} C_j \right)] \end{aligned}$$

Again, we rearrange the order of summation to obtain

$$b_2 = \sum_{j=2}^{N} C_j \sum_{l=j}^{N} R_l \sum_{i=1}^{j-1} C_i \sum_{d=i}^{j-1} R_d + \sum_{j=1}^{N} C_j \sum_{l=j}^{N} L_l \tag{24}$$

Finally, a similar analysis yields

$$b_3 = b_3^{N+1} = R_N (\sum_{j=1}^{N} C_j \cdot b_2^{j-1}) + L_N (\sum_{j=1}^{N} C_j \cdot b_1^{j-1}) + b_3^N$$

from which

$$b_3 = [R_N \left(\sum_{j=1}^{N} C_j \left(\sum_{p=2}^{j-1} C_p \sum_{l=p}^{j-1} R_l \sum_{i=1}^{p-1} C_i \sum_{d=i}^{p-1} R_d + \sum_{p=1}^{j-1} C_p \sum_{l=p}^{j-1} L_l \right) \right) + R_{N-1} ...]$$

$$
\begin{aligned}
&+[L_N\left(\sum_{j=1}^{N} C_j\left(\sum_{p=1}^{j-1} C_p \sum_{l=p}^{j-1} R_l\right)\right) + L_{N-1}...] \\
= \; &[\sum_{q=3}^{N} R_q\left(\sum_{j=1}^{q} C_j\left(\sum_{p=2}^{j-1} C_p \sum_{l=p}^{j-1} R_l \sum_{i=1}^{p-1} C_i \sum_{d=i}^{p-1} R_d + \sum_{p=1}^{j-1} C_p \sum_{l=p}^{j-1} L_l\right)\right)] \\
&+[\sum_{q=3}^{N} L_q\left(\sum_{j=1}^{N} C_j\left(\sum_{p=1}^{j-1} C_p \sum_{l=p}^{j-1} R_l\right)\right)]
\end{aligned}
$$

Again rearranging the variables in the first two summations, we obtain

$$
\begin{aligned}
b_3 \; = \; &\sum_{j=3}^{N} C_j \sum_{q=j}^{N} R_q \sum_{p=2}^{j-1} C_p \sum_{l=p}^{j-1} R_l \sum_{i=1}^{p-1} C_i \sum_{d=i}^{p-1} R_d + \sum_{j=3}^{N} C_j \sum_{q=j}^{N} R_q \sum_{p=1}^{j-1} C_p \sum_{l=p}^{j-1} L_l \\
&+ \sum_{j=3}^{N} C_j \sum_{q=j}^{N} L_q \sum_{p=1}^{j-1} C_p \sum_{l=p}^{j-1} R_l
\end{aligned} \tag{25}
$$

and in general, b_k is given by

$$
b_k = b_k^{N+1} = R_N(\sum_{j=1}^{N} C_j \cdot b_{k-1}^{j-1}) + L_N(\sum_{j=1}^{N} C_j \cdot b_{k-2}^{j-1}) + b_k^N
$$

The coefficients of the s terms for a segmented RC model are obtained by substituting $L = 0$ in the above equations for b_1, b_2 and b_3, i.e.:

$$
\begin{aligned}
b_1 \; &= \; \sum_{j=1}^{N} C_j \sum_{i=j}^{N} R_i \\
b_2 \; &= \; \sum_{j=2}^{N} C_j \sum_{l=j}^{N} R_l \sum_{i=1}^{j-1} C_i \sum_{d=i}^{j-1} R_d \\
b_3 \; &= \; \sum_{j=3}^{N} C_j \sum_{q=j}^{N} R_q \sum_{p=2}^{j-1} C_p \sum_{l=p}^{j-1} R_l \sum_{i=1}^{p-1} C_i \sum_{d=i}^{p-1} R_d
\end{aligned} \tag{26}
$$

Appendix B: Calculation of Moments from the Transfer Function Polynomial

Consider the system transfer function given in Equation (1),

$$H(s) = K\frac{1 + a_1 s + a_2 s^2 + a_3 s^3 + ...}{1 + b_1 s + b_2 s^2 + b_3 s^3 + ...}$$

Considering the denominator polynomial and expanding as an infinite series, we have

$$\begin{aligned} G(s) &= (1 + b_1 s + b_2 s^2 + b_3 s^3 + b_4 s^4 + ...)^{-1} \\ &= [1 - (b_1 s + b_2 s^2 + b_3 s^3 + b_4 s^4 + ...) + (b_1 s + b_2 s^2 + b_3 s^3 + b_4 s^4 + ...)^2 \\ &\quad -(b_1 s + b_2 s^2 + b_3 s^3 + b_4 s^4 + ...)^3 + ...] \\ &= \left(1 - b_1 s + (b_1^2 - b_2)s^2 - (b_3 + b_1^2 - 2b_1 b_2)s^3 + ...\right) \end{aligned} \tag{27}$$

Therefore,

$$\begin{aligned} H(s) &= K(1 + a_1 s + a_2 s^2 + a_3 s^3 + ...)\left(1 - b_1 s + (b_1^2 - b_2)s^2 - (b_3 + b_1^2 - 2b_1 b_2)s^3 + ...\right) \\ &= K[1 + s(a_1 - b_1) + s^2(a_2 - a_1 b_1 + b_1^2 - b_2) \\ &\quad +s^3(a_3 - a_2 b_1 + a_1(b_1^2 - b_2) - b_3 - b_1^3 + 2b_1 b_2) + ...] \end{aligned}$$

Applying the definition of moments (Equation (4)), we obtain

$$\begin{aligned} M_0 &= K \\ M_1 &= K(b_1 - a_1) \\ M_2 &= K(a_2 - a_1 b_1 + b_1^2 - b_2) \\ M_3 &= K\left(b_1^3 + b_3 - 2b_1 b_2 - a_3 + a_2 b_1 - a_1(b_1^2 - b_2)\right) \\ M_4 &= K\left(a_4 - a_3 b_1 + a_2(b_1^2 - b_2) + a_1(b_1^2 + b_3 - 2b_1 b_2) + b_1^4 + b_2^2 + 2b_1 b_3 - b_4 - 3b_1^2 b_2\right) \end{aligned}$$

Recall that we are interested in the special case where the numerator polynomial is constant, i.e., all $a_i = 0$, so that the transfer function is of form

$$H(s) = \frac{1}{1 + b_1 s + b_2 s^2 + b_3 s^3 + ...}$$

and the moments are given by

$$\begin{aligned} M_0 &= 1 \\ M_1 &= b_1 \\ M_2 &= b_1^2 - b_2 \\ M_3 &= b_1^3 + b_3 - 2b_1 b_2 \\ M_4 &= b_1^4 + b_2^2 + 2b_1 b_3 - b_4 - 3b_1^2 b_2 \end{aligned} \tag{28}$$

Appendix C: Convergence of the Coefficients of s^2 and s^3

In this Appendix, we show that the uniform distributed representation of an RC line by **L** segments will converge to the correct values of b_1, b_2 and b_3. As noted above, Sakurai [Sak83] has shown the analogous result for uniform distributed **T** and Π representations, using $ABCD$ matrix representation. His method of derivation leads to the observation "It is difficult to obtain the counterpart of (B8) for the **L** ladder circuit" ([Sak83], p. 425), but he however notes that "it is obvious that Π, **T** and **L** ladder circuits coincide ... if infinite blocks are connected." Here, we show that the desired derivation can be obtained by directly manipulating the summations given in Appendix A.

Case 1: From Equation (26), the coefficient of s is given by

$$b_1 = \sum_{j=1}^{N} C_j \sum_{i=j}^{N} R_i$$

For N uniform distributed **L** segments,

$$\begin{aligned} b_1 &= \sum_{j=1}^{N} \frac{C}{N} \sum_{i=j}^{N} \frac{R}{N} \\ &= \frac{RC}{N^2} \sum_{j=1}^{N} (N - j + 1) \\ &= \frac{RC}{2} \frac{(N+1)}{N} \end{aligned}$$

and thus

$$\lim_{N \to \infty} b_1 = \frac{RC}{2}.$$

Case 2: Similarly, from Equation (26) the coefficient of s^2 is given by

$$b_2 = \sum_{j=2}^{N} C_j \sum_{l=j}^{N} R_l \sum_{i=1}^{j-1} C_i \sum_{d=i}^{j-1} R_d$$

For N uniform distributed **L** segments, the last two summations are in the same form as in the equation for b_1. Therefore,

$$\sum_{i=1}^{j-1} C_i \sum_{d=i}^{j-1} R_d = \frac{RC}{N^2} \frac{j(j-1)}{2}$$

Using the above result in the expression for b_2,

$$
\begin{aligned}
b_2 &= \sum_{j=2}^{N} \frac{C}{N} \sum_{l=j}^{N} \frac{R}{N} \left(\frac{RC}{N^2} \frac{j(j-1)}{2} \right) \\
&= \frac{(RC)^2}{N^2} \sum_{j=2}^{N} (N-j+1) \left(\frac{RC}{N^2} \frac{j(j-1)}{2} \right) \\
&= \frac{(RC)^2}{N^4} \sum_{j=2}^{N} \frac{(N-j+1)j(j-1)}{2} \qquad (*) \\
&= \frac{(RC)^2}{2N^4} \sum_{k=1}^{N-1} (N-k)(k+1)k \\
&= \frac{(RC)^2}{2N^4} \sum_{k=1}^{N-1} \left[Nk^2 - k^3 + Nk - k^2 \right]
\end{aligned}
$$

In the limit, summations involving the lower-order terms Nk and k^2 will vanish. We can use the well-known formulas for $S_k(n)$, i.e., the sum of the k^{th} powers $1^k + 2^k + \ldots + n^k$, to read off the solutions (see, e.g., [GKP89], page. 269),

$$
\begin{aligned}
b_2 &= \frac{(RC)^2}{2N^4} \left[(N-1) \left(\frac{1}{3}(N-1)^3 - \frac{1}{2}(N-1)^2 + \frac{1}{6}(N-1) \right) - \left(\frac{1}{4}N^4 - \frac{1}{2}N^3 + \frac{1}{4}N^2 \right) \right] \\
&\approx \frac{(RC)^2}{2N^4} \left[\frac{1}{3}(N-1)^4 - \frac{1}{4}N^4 \right]
\end{aligned}
$$

Thus, in the limit

$$
\lim_{N \to \infty} b_2 = \frac{(RC)^2}{24}.
$$

The same analysis from **Case 1** can be used to prove that the inductance term in b_2 for RLC segments (Equation (24)) also converges to

$$
\lim_{N \to \infty} \sum_{j=1}^{N} C_j \sum_{l=j}^{N} L_l \to \frac{LC}{2}.
$$

Case 3: Finally, we consider the coefficient of the s^3 term given in Equation (26),

$$
b_3 = \sum_{j=3}^{N} C_j \sum_{q=j}^{N} R_q \left(\sum_{p=2}^{j-1} C_p \sum_{l=p}^{j-1} R_l \sum_{i=1}^{p-1} C_i \sum_{d=i}^{p-1} R_d \right)
$$

For uniform segments, notice that the the last four summations have been solved in our analysis of the b_2 expression namely,

$$
\sum_{p=2}^{j-1} C_p \sum_{l=p}^{j-1} R_l \sum_{i=1}^{p-1} C_i \sum_{d=i}^{p-1} R_d = \frac{(RC)^2}{2N^4} \sum_{k=1}^{j-2} (j-1-k)(k+1)k
$$

from which

$$\begin{aligned} b_3 &= \sum_{j=3}^{N} \frac{C}{N} \sum_{q=j}^{N} \frac{R}{N} \left[\frac{(RC)^2}{2N^4} \sum_{k=1}^{j-2} (j-1-k)(k+1)k \right] \\ &= \frac{(RC)^3}{2N^6} \left[\sum_{j=3}^{N} (N-j+1) \sum_{k=1}^{j-2} (j-1-k)(k+1)k \right] \\ &= \frac{(RC)^3}{2N^6} \left[\sum_{j=1}^{N-2} (N-j-1) \sum_{k=1}^{j-2} (j-1-k)(k+1)k \right]. \end{aligned}$$

Evaluating the inner summation,

$$\begin{aligned} \sum_{k=1}^{j-2} (j-1-k)(k+1)k &= \sum_{k=1}^{j-2} (j-k)(k^2+k) - (K^2+k) \\ &= \sum_{k=1}^{j-2} (jk^2 + jk - k^3 - 2k^2 - k) \end{aligned}$$

Again using the formulas for $S_k(n)$ and retaining only the leading terms,

$$\sum_{k=1}^{j-2} (j-1-k)(k+1)k \approx \frac{j^4}{12} - \frac{j^3}{6},$$

from which

$$b_3 \approx \frac{(RC)^3}{2N^6} \left[\sum_{j=1}^{N-2} (N-j-1)(\frac{j^4}{12} - \frac{j^3}{6}) \right].$$

Again eliminating all the lower-order terms in the limit, we obtain

$$\begin{aligned} b_3 &\approx \frac{(RC)^3}{2N^6} \left[\sum_{j=1}^{N-2} (\frac{Nj^4}{12} - \frac{j^5}{12}) \right] \\ &\approx \frac{(RC)^3}{2N^6} [\frac{1}{60} N^6 - \frac{1}{72} N^6] \\ &\rightarrow \frac{(RC)^3}{720}. \end{aligned}$$

Appendix D: Calculation of Voltage Response Using Moments

The transfer function of the system considering two dominant poles is

$$H(s) = \frac{k_1}{s - s_1} + \frac{k_2}{s - s_2}$$

where s_1, s_2 are the poles and k_1, k_2 are the coefficients corresponding to the poles.

Assuming a step input, $V_{in}(t) = V_0 u(t)$, $V_{in}(s) = \frac{V_0}{s}$, the output voltage given by

$$V_{out}(s) = V_0 \frac{H(s)}{s}$$

Applying partial fractions and taking the inverse Laplace transform:

$$V_{out}(t) = \left(-(\frac{k_1}{s_1} + \frac{k_2}{s_2}) + \frac{k_1}{s_1} e^{s_1 t} + \frac{k_2}{s_2} e^{s_2 t} \right)$$

Now using the following boundary conditions one can solve for s_1, s_2, k_1, k_2,

$$V_{out}(t = 0) = 0, V'_{out}(t = 0) = 0 \tag{29}$$

Therefore,

$$-(\frac{k_1}{s_1} + \frac{k_2}{s_2}) = 1$$
$$k - 1 + k_2 = 0$$

Now by applying the definition of moments from Equation (4) to the two-pole transfer function, we get

$$(\frac{k_1}{s_1^2} + \frac{k_2}{s_2^2}) = M_1$$
$$(\frac{k_1}{s_1^3} + \frac{k_2}{s_2^3}) = M_2$$

and solving above equations yields

$$s_{1,2} = \frac{2}{-M_1 \pm \sqrt{4M_2 - 3M_1^2}}$$

$$k_1 = -k_2 = -\frac{1}{\sqrt{4M_2 - 3M_1^2}}$$

Note that the poles of the system should be always in the left half of the $s-$plane for stable systems. The voltage response can be calculated for both real and complex poles as follows:

Case 1: Real Poles.

From the above equations,

$$k_1 = -\frac{s_1 s_2}{s_2 - s_1}$$

and

$$k_2 = \frac{s_1 s_2}{s_2 - s_1}$$

The voltage response for real poles is

$$V_{out}(t) = V_0(1 - \frac{s_2}{s_2 - s_1}e^{s_1 t} - \frac{s_1}{s_1 - s_2}e^{s_2 t}) \tag{30}$$

Note that this is exactly the same as in [ZSTGC92].

Case 2: Complex Poles.

Since the poles are complex we can express them in the form $s_1 = -\alpha + \jmath\beta$ and $s_2 = -\alpha - \jmath\beta$.

The voltage response is

$$\begin{aligned} V_{out}(t) &= V_0\left[1 - \frac{s_2}{s_2 - s_1}e^{s_1 t} - \frac{s_1}{s_1 - s_2}e^{s_2 t}\right] \\ &= V_0\left[1 - \frac{e^{-\alpha t}}{2}\left((1 + \frac{\alpha}{\jmath\beta})e^{\jmath\beta t} + (1 - \frac{\alpha}{\jmath\beta})e^{-\jmath\beta t}\right)\right] \\ &= V_0\left[1 - e^{-\alpha t}(cos(\beta t) + \frac{\alpha}{\beta}sin(\beta t))\right] \\ &= V_0\left[1 - \frac{\sqrt{\alpha^2 + \beta^2}}{\beta}e^{-\alpha t}sin(\beta t + \rho)\right] \end{aligned}$$

where $\rho = tan^{-1}(\frac{\beta}{\alpha})$ and

$$\alpha = \frac{M_1}{2(M_1^2 - M_2)}$$

$$\beta = \frac{\sqrt{3M_1^2 - 4M_2}}{2(M_1^2 - M_2)}$$

Appendix E: Three Non-Uniform RC Segment Model

In this Appendix we will try to obtain the parameters for three non-uniform RC segment model in terms of the distributed RC line parameters.

The open-ended transfer function for distributed RC line is obtained by substituting $L = 0$ in Equation (6),

$$H(s) = \frac{1}{1 + \frac{RC}{2}s + \frac{(RC)^2}{24}s^2 + \frac{(RC)^3}{720}s^3 + ...} \tag{31}$$

The open-ended transfer function for three uniform L-type RC segments (Figure 3) is given by

$$H_{eq}(s) = \frac{1}{1 + b_1 s + b_2 s^2 + b_3 s^3} \tag{32}$$

where

$$\begin{aligned} b_1 &= R_1(C_1 + C_2 + C_3) + R_2(C_2 + C_3) + R_3 C_3 \\ b_2 &= R_1 R_2 C_1 C_2 + R_1 R_3 C_1 C_3 + R_2 R_3 C_2 C_3 + R_1 R_3 C_2 C_3 + R_1 R_2 C_1 C_3 \\ b_3 &= R_1 R_2 R_3 C_1 C_2 C_3 \end{aligned}$$

Since the three segment RC model should match the distributed RC line transfer function up to the third moment (see Appendix B), comparing the coefficients of s, s^2, s^3 in Equation (31) and (32), we obtain the following equations

$$R_1(C_1 + C_2 + C_3) + R_2(C_2 + C_3) + R_3 C_3 = \frac{RC}{2} \tag{33}$$

$$R_1 R_2 C_1 C_2 + R_1 R_3 C_1 C_3 + R_2 R_3 C_2 C_3 + R_1 R_3 C_2 C_3 + R_1 R_2 C_1 C_3 = \frac{(RC)^2}{24} \tag{34}$$

$$R_1 R_2 R_3 C_1 C_2 C_3 = \frac{(RC)^3}{720} \tag{35}$$

Clearly there is no unique solution if we try to solve for the six variable parameters of the model given in (Figure 3) using the above three equations. Using the approach given in [Raj74] we can obtain more information by calculating the open-circuit input impedance for both the distributed RC line and for the three segment model.

The open-circuit input impedance, z_{11} of the distributed RC line is given by [GK68]

$$z_{11} = \frac{1 + \frac{RC}{2!}s + \frac{(RC)^2}{4!}s^2 + \frac{(RC)^3}{6!} + \ldots}{\frac{C}{1!}s + \frac{RC^2}{3!}s^2 + \frac{R^2C^3}{5!}s^3 + \ldots} \tag{36}$$

The open-circuit input impedance for three uniform **L**-type RC segments is

$$(z_{11})_{eq} = \frac{1 + b_1 s + b_2 s^2 + b_3 s^3}{a_1 s + a_2 s^2 a_3 s^3} \tag{37}$$

where the numerator polynomial (i.e. the variables b_i's) is exactly same as the the denominator polynomial of the open-ended transfer function given in Equation (32) and the coefficients a_i's are

$$\begin{aligned} a_1 &= C_1 + C_2 + C_3 \\ a_2 &= R_2C_1C_2 + R_3C_1C_3 + R_2C_1C_3 + R_3C_2C_3 \\ a_3 &= R_2R_3C_1C_2C_3 \end{aligned}$$

Comparing the coefficients of s, s^2, s^3 in the denominator of the Equation (36) and (37) yields the following equations,

$$C_1 + C_2 + C_3 = C \tag{38}$$

$$R_2C_1C_2 + R_3C_1C_3 + R_2C_1C_3 + R_3C_2C_3 = \frac{RC^2}{6} \tag{39}$$

$$R_2R_3C_1C_2C_3 = \frac{R^2C^3}{120} \tag{40}$$

Note that the by comparing the numerator of the Equation (36) and (37) we get the same equations as (33) - (35).

Since the sum of all the resistances should be equal to the total line resistance,

$$R_1 + R_2 + R_3 = R \tag{41}$$

Clearly we can not solve for the six unknown parameters $R_1, R_2, R_3, C_1, C_2, C_3$ using these seven overspecified equations. Thus, we have obtained values for these parameters by using numerical techniques to minimize the squared error in the coefficients b_1, b_2, b_3.

The above analysis can be extended to RLC segment models by replacing all the resistances R_i's by $R_i + sL_i$ and then comparing the corresponding coefficients s's of the open-circuit input impedance numerator and denominator polynomials.

References

[BKR93] K. D. Boese, A. B. Kahng and G. Robins, "High-Performance Routing Trees With Identified Critical Sinks", *Proc. 30th ACM/IEEE Design Automation Conf.*, June 1993, pp. 182-187.

[CLZ93] J. Cong, K. S. Leung and D. Zhou, "Performance-Driven Interconnect Design Based on Distributed RC Delay Model", *Proc. 30th ACM/IEEE Design Automation Conf.*, June 1993, pp. 606-611.

[Dwo79] L. N. Dworsky, *Modern Transmission Line Theory and Applications*, Wiley, 1979.

[E48] W. C. Elmore, "The Transient Response of Damped Linear Networks with Particular Regard to Wideband Amplifiers", *Journal of Applied Physics* 19, Jan. 1948, pp. 55-63.

[Eda93] M. Edahiro, "A Clustering-Based Optimization Algorithm in Zero-Skew Routings", *Proc. 30th ACM/IEEE Design Automation Conf.*, June 1993, pp. 612-616.

[GZ93] D. S. Gao, D. Zhou, "Propagation Delay in RLC Interconnection Networks", *Int. Symposium on Circuits and Systems*, May 1993, pp. 2125-2128.

[GKP89] R. L. Graham, D. E. Knuth and O. Patashnik, *Concrete Mathematics*, Addison-Wesley, 1989.

[Hor84] M. A. Horowitz, "Timing Models for MOS Circuits", *PhD Thesis*, Stanford University, Jan. 1984.

[GK68] M. S. Ghausi and J. J. Kelly, *Introduction to Distributed-Parameter Networks: With Application to Integrated Circuits*, New York: Holt, Rinehart and Winston, 1968.

[Kum80] U. Kumar, "Modeling of Distributed Lossless and Lossy Structures: A Review", *IEEE Circuits and Systems Magazine* 2(3), 1980, pp. 12-16.

[McC89] S. P. McCormick, "Modeling and Simulation of VLSI Interconnections with Moments", *PhD Thesis*, MIT, June 1989.

[RPH83] J. Rubinstein, P. Penfield and M. A. Horowitz, "Signal Delay in RC Tree Networks", *IEEE Trans. on CAD* 2(3), July 1983, pp. 202-211.

[Sak83] T. Sakurai, "Approximation of Wiring Delay in MOSFET LSI", *IEEE Journal of Solid-State Circuits*, Aug. 1983, Vol.18, No.4, pp. 418-426.

[WE88] N. Weste and K. Eshraghian, *Principles of CMOS VLSI Design: A systems Perspective*, Addison-Wesley, 1988.

[Raj74] Y. V. Rajput, "Modelling Distributed *RC* Lines for the Transient Analysis of Complex Networks", *Int. Journal of Electronics* 36(5), 1974, pp. 709-717.

[ZSTGC92] D. Zhou, S. Su, F. Tsui, D. S. Gao and J. S. Cong, "Analysis of Tree of Transmission Lines", *Computer Science Department, Tech. Report CSD-920010, UCLA*, March 1992 (also to appear as "Simplified Synthesis of Transmission Lines with A Tree Structure", *Intl. Journal of Analog Integrated Circuits and Signal Processing (Special Issue on High-Speed Interconnects)*, 1993).

[ZPK91] D. Zhou, F. P. Preparata and S. M. Kang, "Interconnection Delay in Very High-Speed VLSI", *IEEE Trans. on Circuits and Systems* 38(7), July 1991, pp. 779-790.

[ZTG93] D. Zhou, F. Tsui and D. S. Gao, "High Performance Multichip Interconnection Design", *Proceedings of the 4th ACM/SIGDA VLSI Physical Design Workshop*, April 1993, pp. 32-43.